Optics and Laser Technology 108 (2018) 542–550

Contents lists available at ScienceDirect

Optics and Laser Technology

journal homepage: www.elsevier.com/locate/optlastec

Full length article

Experimental study of optical frequency comb generation in gain-switched semiconductor lasers

Alejandro Rosado [a,*], Antonio Pérez-Serrano [a], José Manuel G. Tijero [a], Ángel Valle [b], Luis Pesquera [b], Ignacio Esquivias [a]

[a] CEMDATIC – E.T.S.I Telecomunicación, Universidad Politécnica de Madrid (UPM), 28040 Madrid, Spain
[b] Instituto de Física de Cantabria, (CSIC-Universidad de Cantabria), 39005 Santander, Spain

ARTICLE INFO

Article history:
Received 25 May 2018
Accepted 16 July 2018

Keywords:
Semiconductor lasers
Gain switching
Optical injection
Optical Frequency Combs

ABSTRACT

A systematic experimental study of the generation of Optical Frequency Combs (OFCs) by gain switching two types of edge emitting semiconductor lasers (Distributed Feedback and Discrete Mode) is presented. High resolution spectral measurements together with linewidth characterization and the analysis of the temporal profiles and the radio-frequency spectra are used to evaluate the evolution of the quality of the OFCs, as a function of the driving conditions. Different types of emission spectra are identified. The physical origin of the OFC properties is discussed. The results indicate that the driving conditions rather than the device properties determine the OFC quality. The optical injection is demonstrated to either improve or deteriorate the quality of the OFCs generated by gain switching, depending on the injection conditions.

1. Introduction

In the last decades, Optical Frequency Combs (OFCs) and their numerous applications have been the subject of an enormous and increasing research effort. Some of the main applications justifying this interest are: metrology [1], radio-photonics [2], optical communications [3,4], molecular spectroscopy [5], arbitrary waveform generation [6] and LIDAR [7].

More recently semiconductor lasers have come on the scene of the OFC sources by exhibiting their usual credentials: high efficiency, low cost and small footprint. Among the three main strategies for generating OFCs from semiconductor lasers, namely mode locking, gain switching and electro-optic modulation, gain switching has attracted specific attention due to its easy implementation, high flexibility in the selection of the repetition frequency and low losses. Gain switching is a technique initially conceived for short optical pulse generation. As such, it is realized by superimposing a radio-frequency (RF) current to a direct bias current such that only the first spike of the relaxation oscillations is excited at the onset of laser operation while the subsequent peaks are cut off by the switch off period of the RF driving current [8,9]. However, throughout this work, and following the usual practice in OFC generation from semiconductor lasers, we will refer to as gain switching any large signal modulation process, no matter the laser is actually switched off or just modulated.

Though spectral aspects and coherence of the train of gain switching pulses were acknowledged as important for some applications [10], until recently more attention had been paid to the temporal aspects than to the inherent frequency comb character of the pulses, partially due to the lack of optical spectrum analyzers with enough resolution. It was not until 2009 when Anandarajah et al. [11] demonstrated the OFC generation from gain-switched Discrete Mode lasers (DMLs). The performance of the OFCs generated from these lasers in a Differential Phase Shift Keyed transmission system was compared with the performance of gain-switched conventional Distributed Feedback (DFB) lasers. It was claimed a superior performance of the first that was attributed to a lower phase noise. Since then, the generation of OFCs by gain switching edge-emitting single-mode lasers has been the subject of a good deal of application-driven research. The main targeted applications are in the domain of the optical communications. The state of the art in these applications has been very recently reviewed by Imran et al. in a excellent tutorial ([4] and references therein). In some interesting contributions to this field the OFCs have been referred to as multiwavelength sources and the generation method as direct modulation [12,13]. Other applications such as dual comb spectroscopy have also been proved attainable by OFCs generated by gain switching edge-emitting laser diodes [14]. It is also worth mentioning the recent progresses made towards the integration of these devices [15–17]. Regarding Vertical Cavity Surface

* Corresponding author.
E-mail address: alejandro.rosado@upm.es (A. Rosado).

https://doi.org/10.1016/j.optlastec.2018.07.038
0030-3992/

Emitting Lasers (VCSELs), the generation of OFCs by gain switching these lasers has also been demonstrated [18] and a significant enlargement of the frequency span by additional non-linear techniques has been shown [19,20]. It has been demonstrated that the two orthogonal polarizations generate correlated OFCs and the polarization dynamics has been theoretical and experimentally analyzed [21,22].

Coming back to edge-emitting lasers, the phase noise/linewidth, the jitter, the modulation bandwidth and the frequency chirp have been analyzed as related key issues affecting the performance in the targeted applications of the OFCs generated by gain switching these lasers [23–26]. However, the generation of OFCs by gain switching lacks a systematic study of the effect of the switching conditions on the characteristics of the generated OFCs, in line with the analysis performed in [21] for the OFCs generated by gain switching VCSELs. Only the role of the modulation frequency has been studied in a short range of frequencies around the relaxation oscillation frequency [27].

On the other hand, the effect of external optical injection (OI) in semiconductor lasers in single-mode CW operation has been extensively studied and the appearance of a wide variety of induced dynamical regimes, including injection locking, four-wave mixing, self-pulsations and chaotic behaviour through a period-doubling cascade has been described [28]. Regarding gain switched lasers, external OI has been demonstrated to reduce related detrimental characteristics such as phase noise, time jitter, frequency chirp and relative intensity noise (RIN), thus contributing to improve the spectral quality of the OFCs [29,23,30,25,24,31]. In particular, Anandarajah et al. [30] demonstrated for the first time that the broad noisy spectra of a gain-switched DFB laser can be transformed into a high quality OFC by external optical injection. Furthermore, an increase of the maximum attainable frequency spacing of the comb tones by strong OI has been reported [32] and a large tunability range, spanning the entire C-band, has been demonstrated by tunable injection of the combs generated by gain switching in Fabry-Perot laser diodes [33]. Therefore, OI has become a usual complement for OFCs generated by gain switching when improved performance is required. And yet, again, a systematic analysis of the effect of the OI conditions on the properties of the injected combs has not been reported. For example, though expected, the fact that OI may not only improve the properties of the injected combs but also worsen them depending on the injection conditions has not been experimentally reported and only recently a simulation based exploration of the injection power and detuning conditions for efficient locking has been published [34].

In this paper we report on a systematic experimental study of the effect of the gain switching conditions namely, the bias current and the amplitude and frequency of the RF current, on the temporal and spectral characteristics of the OFCs generated by gain switching two representative edge-emitting single-mode lasers, a DFB laser and a DML. The combined information provided by the optical spectra, the temporal profiles, the electrical RF spectra and linewidth measurements is used for ascertaining the origin of the comb characteristics and their evolution as a function of a wide range of switching conditions, including conditions at which no discernible combs are generated. The results provide guidelines for selecting the suitable switching conditions for specific OFC characteristics. The study is complemented with an exploration of the effect of the OI under specific conditions of fixed detuning and increasing power, and fixed power and variable detuning. The effects are analyzed on both, a noisy broad spectrum and also a good OFC spectrum of the free running gain-switched laser. The analysis reported in this work reveals the relevant role of the dynamic and adiabatic chirp in the evolution of the spectra as a function of the switching conditions and the role of the adiabatic chirp on the frequency modulation (FM) at low switching frequencies. Our work clearly shows that the coherence of the combs relies on a non-complete extinction of the stimulated emission between successive pulses. Therefore, the spectral width of the combs increases as a function of the RF amplitude provided that the bias current is big enough to prevent total extinction of the stimulated emission. The work also shows that the characteristics of the OFCs basically depend on the switching conditions rather than on the type of cavity or other internal parameters of the laser, such that DFB lasers and DMLs behave alike when similarly switched. Finally, we provide experimental evidence of both, the improvement by OI of the spectral quality of noisy broad spectra of non-injected gain-switched lasers, but also the worsening of the quality of the OFCs by OI in a wide range of injection conditions.

The paper is organized as follows. In Section 2, relevant details of the lasers and the experimental setups are provided and the parameters used for characterizing the spectra are defined. Section 3 is devoted to the presentation and discussion of the experimental results. In Section 3.1 the CW characterization of the lasers is reported, while Section 3.2 is devoted to the systematic analysis of the OFC generation by gain switching under a wide range of conditions and Section 3.3 focuses on the discussion of the effects of the OI on the characteristics of the OFCs. Finally, the conclusions are presented in Section 4.

2. Experimental details

Two different types of high bandwidth 1550 nm commercial lasers were used to generate the OFCs: a DFB laser from Gooch & HouseGo and a DML from Eblana Photonics. The nominal modulation bandwidths of the devices were 9 and 10 GHz, respectively. Both diode lasers were packaged in 7-pin butterfly with high frequency input connectors and they had no built-in optical isolator in order to allow external optical injection.

Fig. 1 shows the schematics of the experimental setup for the characterization of the OFCs generated by gain switching with (or without) OI. A tunable laser (Pure Photonics PPCL300), with a narrow linewidth (75 kHz), was used as a master laser (ML). The slave laser (SL), a DFB laser or a DML, is driven by a superposition of two currents, a CW bias current I_{bias}, provided by a current source (Arroyo 4205) and a sinusoidal modulation current at a frequency f_m, provided by a RF/Microwave signal generator (Rohde & Schwarz SMB100A). The input impedance of the lasers Z_L, is around 50 Ω at frequencies below 1 GHz and then the peak amplitude of the RF current is around $\frac{\sqrt{2}V_{RF}}{Z_L}$, where V_{RF} is the rms voltage at the input of both lasers. An optical circulator is used to inject the out-

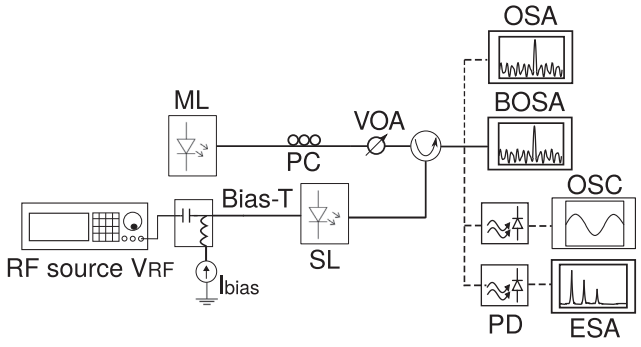

Fig. 1. Schematic diagram of the experimental setup. The master laser (ML) is a tunable laser while the slave laser (SL) is either a DFB or a DML laser. PC: Polarization controller, VOA: Variable Optical Attenuator, BOSA: Brillouin Optical Spectrum Analyzer, OSA: Optical Spectrum Analyzer, OSC: Oscilloscope, ESA: Electric Spectrum Analyzer, PD: Photodetector.

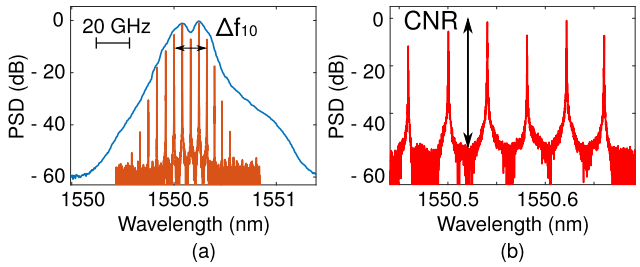

Fig. 2. (a) Spectrum of an OFC measured with the OSA (blue) and with the BOSA (red) (I_{bias} = 30 mA, f_m = 5 GHz and V_{RF} = 0.4 V). The arrows indicate the 10 dB spectral width (Δf_{10} = 20 GHz). (b) Closer look at the 1550.4 nm region of the BOSA spectrum. The Carrier-to-Noise Ratio (CNR = 53 dB) is indicated. (For interpretation of the references to colour in this figure legend, the reader is referred to the web version of this article.)

put of the ML into the SL and a polarization controller is used to maximize the coupling between both lasers. The output of the SL is spectrally characterized either with a Brillouin Optical Spectrum Analyzer (BOSA) (Aragon Photonics BOSA 210), with 10 MHz resolution, or with a conventional Optical Spectrum Analyzer (OSA) (ANDO AQ6315) with 6.25 GHz resolution at the lasing wavelength. Temporal traces were acquired with a Digital Signal Analyzer (Tektronix DSA8200) using an optical input module with 20 GHz bandwidth. The electrical frequency spectra were measured with a 45 GHz photodiode (Newfocus 1014) and a 44 GHz Electrical Spectrum Analyzer (ESA) (Agilent E4446).

The advantage of high resolution spectral measurements for the characterization of OFCs is illustrated in Fig. 2(a), where we compare measurements provided by the BOSA and by the OSA of the spectrum of an OFC generated at modulation frequency $f_m = 5$ GHz. The tones of the comb are clearly resolved by the BOSA, while the low resolution of the OSA does not allow resolving the individual tones and therefore the quality of the OFC cannot be characterized. In order to characterize the spectral quality of an OFC we define two parameters: (i) the 10 dB spectral width (Δf_{10}), defined as the frequency difference between the two most sparated tones (at the high and low sides of the optical carrier) which intensity is not more than ten times lower than the intensity of the strongest tone (see Fig. 2(a)); (ii) the Carrier-to-Noise Ratio (CNR), defined as the average value of the ratio between the intensities of those tones within Δf_{10} and the noise level at frequencies between adjacent tones. Fig. 2(b) shows a magnified view of the BOSA spectrum in Fig. 2(a), illustrating the value of the CNR.

The Delayed Self-Heterodyne (DSH) technique [35,36] was used to characterize the emission linewidth of the lasers under both conditions. The delay was attained by making the light pass through a 25 km single mode fiber spool and the frequency shift f_s = 80 MHz was achieved by means of an acousto-optic modulator. When the lasers were gain-switched, the emission was filtered through a Fabry-Perot Optical Filter (FFP-TF2, MicronOptics) in order to select a single tone from the OFC.

3. Results and discussion

3.1. CW characterization

The lasers were characterized in CW operation by means of Power-Current characteristics, optical spectra and RIN measurements. The threshold currents, I_{th}, for the DML and the DFB laser are 14.5 mA and 10.5 mA, respectively. The optical spectra of the two devices at 40 mA as measured with the OSA are shown in Fig. 3(a) and (b). The emission wavelength is close to 1550 nm, and the Side Mode Suppression Ratio (SMSR) is around 45 dB and

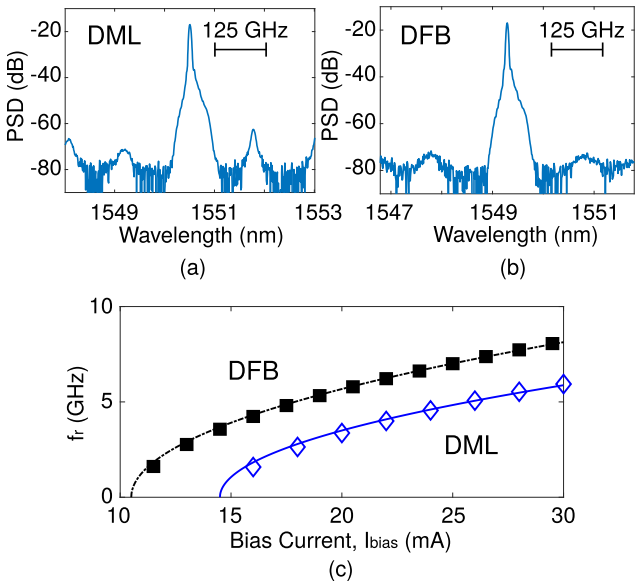

Fig. 3. Optical spectra of the DML (a) and the DFB laser (b) measured with the OSA (I_{bias} = 40 mA). (c) Relaxation oscillation frequency f_r vs I_{bias} for the DML (blue diamonds) and the DFB laser (black solid squares). The lines correspond to the square root dependence (see text). (For interpretation of the references to colour in this figure legend, the reader is referred to the web version of this article.)

53 dB for the DML and the DFB laser, respectively. The SMSR is almost independent of the bias in the case of the DFB laser, while it increases with the bias in the DML.

RIN measurements were used to extract the relaxation oscillation frequency, f_r, and the damping factor, γ, as a function of the bias current by fitting the experimental data to the standard analytical expression [37]. Fig. 3(c) shows the values of f_r vs I_{bias}, which were fitted to the expected dependence $f_r = \sqrt{\chi(I_{bias} - I_{th})}$. The parameter χ was 3.39 and 2.22 GHz^2/mA for the DFB laser and the DML respectively. The extracted damping factor was fitted to $\Gamma = Kf_r^2 + \gamma_0$, yielding similar values of K, around 0.17 ns, for both lasers.

3.2. Gain switching operation

The temporal and spectral responses of the lasers in gain switching operation were characterized for different values of f_m ranging between 100 MHz and 10 GHz. In the following, we will show results at only two relevant frequencies: $f_m = 500$ MHz, within the range used in spectroscopic applications, and $f_m = 5$ GHz, close to the frequencies used in optical communications. The results at other frequencies are qualitatively similar to those presented here.

Fig. 4 shows the temporal traces, the RF spectra and the optical spectra of the DML emission at $f_m = 500$ MHz, I_{bias} = 50 mA (much higher than threshold) and different values of V_{RF}, increasing from left to right. Looking at the temporal traces (upper row), clearly sinusoidal profiles are apparent in Fig. 4(a) and (b), corresponding to a direct modulation of the laser, as the injected current is higher than I_{th} for the entire period. When increasing the modulation amplitude (Fig. 4(c)), a clear distortion of the sinusoid appears, although the laser remains in the on state during the complete modulation period. At the highest modulation amplitude (Fig. 4 (d)) the total injection current becomes lower than I_{th} during the period of negative modulation current and therefore the laser is actually switched-off during this period. During the switch-on period a small gain switching pulse appears followed by a

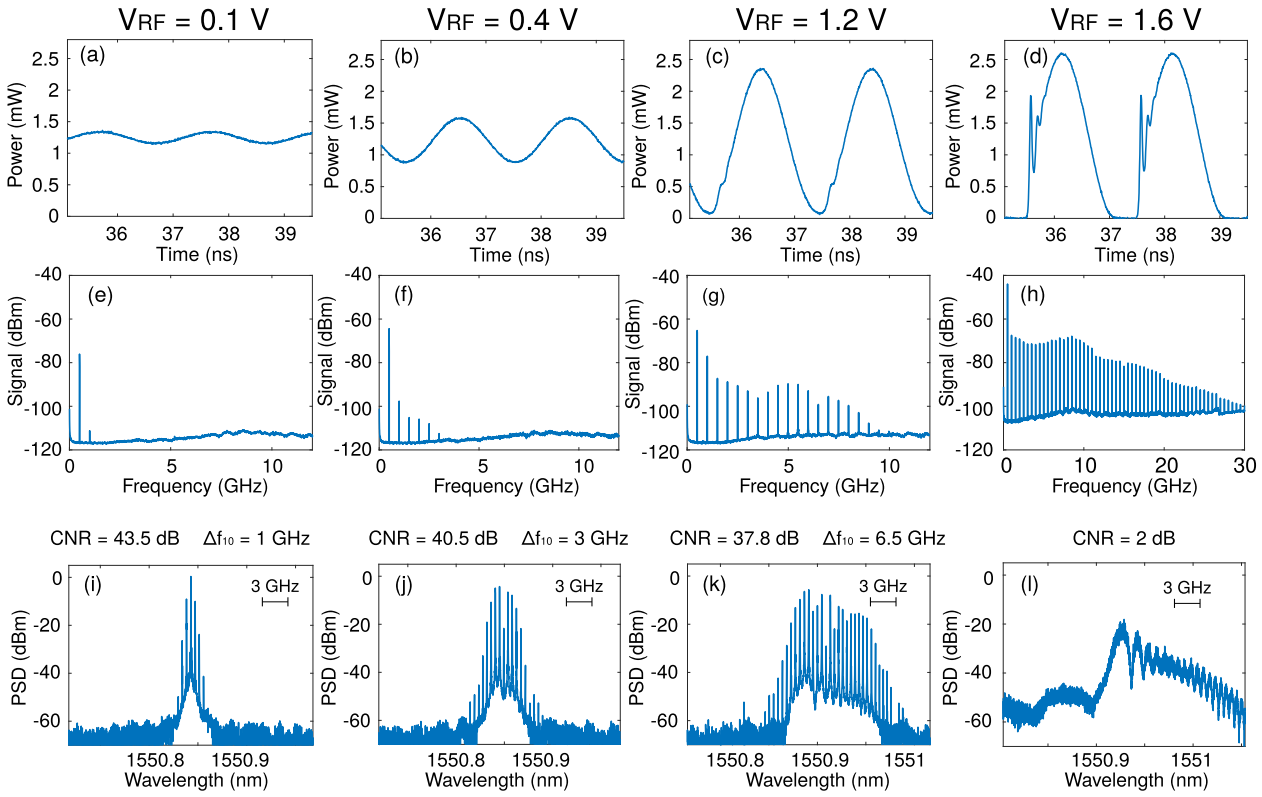

Fig. 4. Temporal traces (upper row), RF spectra (middle row) and optical spectra (lower row) of the DML emission at I_{bias} = 50 mA and f_m = 500 MHz and different values of V_{RF}. Each column corresponds to the value of V_{RF} labelled on the top.

semi-sinusoidal trace corresponding to the positive cycle of the total current. The corresponding RF spectra shown in the second row are logically consistent with the temporal profiles of the output power: a very high ratio between the amplitudes of the first and second harmonics (~15 dB) in Fig. 4(e), corresponding to an almost pure tone, and an increase of the amplitude and number of high order harmonics when increasing the modulation amplitude. However, a significant difference appears at high modulation amplitude, apart from the increased number of harmonics (Fig. 4 (h)). In this case, although the discrete harmonics remain clearly discernible, the level of continuous noise increases above the noise floor. This is consistent with the preservation of the periodic character of the signal and the appearance of an uncorrelated time jitter due to the emergence of the laser signal from the spontaneous emission after the switch-off period. A similar effect has been theoretically analyzed [31,38] and experimentally evidenced [39] for much shorter gain switching pulses at higher modulation frequencies.

The optical spectra in the lower row of Fig. 4 show very different characteristics regarding CNR and Δf_{10}. The results can be understood by considering the combined effect of amplitude modulation (AM) and frequency modulation (FM) caused by the direct intensity modulation [40]. The first one (Fig. 4(i)), corresponding to a small modulation amplitude, shows an almost symmetric spectrum with only three tones within the 10-dB spectral width (Δf_{10} = 1 GHz) and a high CNR = 43.5 dB, which is due to the AM. The second one (Fig. 4(j)) corresponds to a higher modulation amplitude although the trace is still rather sinusoidal. It shows an asymmetric spectrum with seven tones in the 10-dB spectral width, a clear suppression of the central tone and also high CNR = 40.5 dB. The carrier frequency suppression is a typical feature of FM, which can be caused either by carrier or by thermal effects [40]. The carrier modulation induces frequency chirp due to either the dynamic response of the laser during the switching (dynamic chirp), or to the dependence of the carrier density, and hence of the emission wavelength, on the photon density through the non-linear gain saturation (adiabatic chirp) [41]. In this particular case, at a relatively low modulation frequency (500 MHz), we attribute the FM to adiabatic chirp. In the third case (Fig. 4(k)), corresponding to a higher V_{RF}, the optical spectrum shows a much higher number of tones (Δf_{10} = 6.5 GHz) keeping a high CNR. Regarding CNR and Δf_{10}, this is the best OFC obtained at this repetition frequency. However, some tones are partially suppressed and the shape of the spectral envelope shows a depression in the red region. Finally, in the fourth case (Fig. 4(l)), the optical spectrum has a low value of CNR (2 dB) and cannot be considered as a proper OFC with discernible lines. This happens when the modulation amplitude is high enough to switch off the laser and therefore the coherence of the pulses is lost. The subsequent pulses are built up from spontaneously emitted photons with a random initial phase and, in consequence, the CNR is very low. It is interesting to notice that, as mentioned above, in this case, the RF spectrum shows clear harmonics with up to 60 dB peak to noise ratio (Fig. 4(h)) and a narrow linewidth, limited by the equipment resolution (around 1 Hz). This indicates that, although some features in the RF spectra may be indicative of lack of coherence, the coherence of the OFCs should be preferably evaluated by optical measurements.

The temporal traces and the optical spectra at 5 GHz for the DML at constant bias with different modulation amplitudes are shown in Fig. 5. The RF spectra are not shown because they do not provide significant additional information. The observed behavior of the temporal traces and the corresponding spectra is similar, but not identical, to the results at 500 MHz. At low V_{RF} a sinusoidal trace is obtained (Fig. 5(a)). The corresponding optical spectrum (Fig. 5(e)) has a high CNR = 60 dB but a low number of tones. At higher V_{RF} the temporal profile is no longer sinusoidal

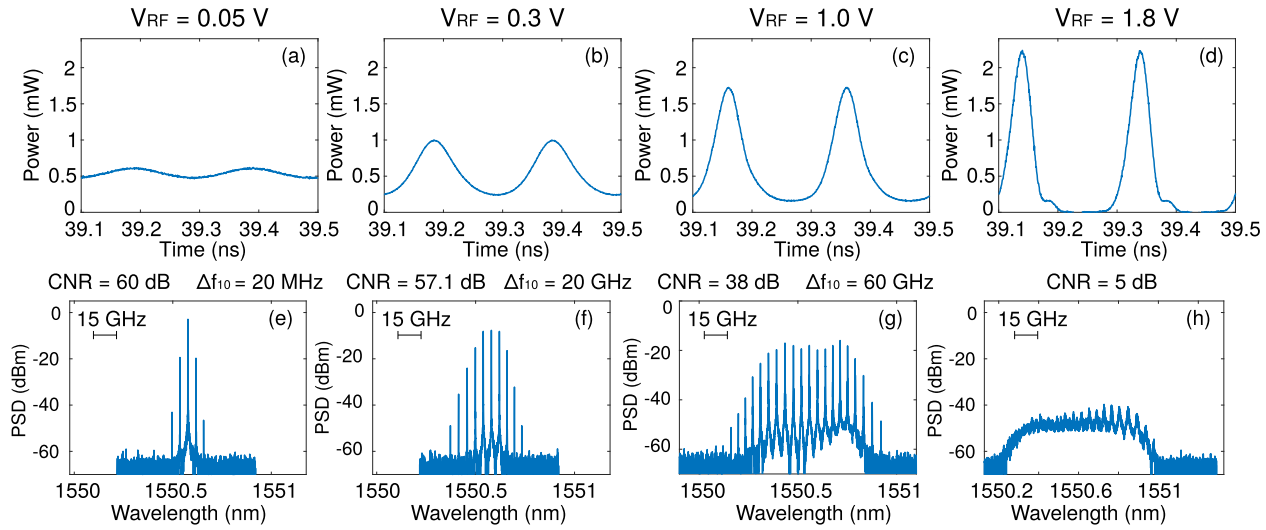

Fig. 5. DML performance dependence on the modulation amplitude V_{RF} for I_{bias} = 30 mA and f_m = 5 GHz. Temporal traces (upper row) and optical spectra (lower row) of the DML emission at I_{bias} = 30 mA, f_m = 5 GHz and different values of V_{RF}. Each column corresponds to the value of the V_{RF} labelled on the top.

and the FM broadens the spectrum that includes a higher number of coherent tones (Fig. 5(b) and (f)). A broader and flatter comb is obtained (Fig. 5(g)) when the intensity of the modulation does not switch-off completely the laser between pulses (Fig. 5(c)). In this case, the spectral width Δf_{10} is 60 GHz and the asymmetric envelope spectrum shows a maximum at the red side. This is the classical shape of gain-switched laser spectra when measured with low spectral resolution [42,43]. We attribute this type of OFC to the dynamic frequency chirp caused by the photon-carrier interaction at frequencies close to the relaxation frequency. Finally, the last column in Fig. 5 corresponds to the highest V_{RF} yielding the narrowest pulses with complete switch-off between pulses, and giving rise to an optical spectrum with no discernible tones (CNR < 5 dB). This type of spectrum in gain-switched lasers has been previously experimentally reported [44,30,27] and simulated [27,31,22]. As discussed in [22,27], in this case the pulses are built-up from spontaneous emission and not from the previous pulse; then the coherence between pulses is lost, and in consequence the spectrum does not show resolved tones.

The transition from high quality coherent OFCs such as that shown in Fig. 5(g) to broad noisy spectra without discernible tones (Fig. 5(h)) has been previously reported by changing the type of device or the operating conditions. In [30,44], a good OFC is obtained in a DML while a broad noisy spectrum is obtained in a DFB laser; in [30] the broad spectrum of the DFB evolves to high CNR tones by optical injection; in [27] the transition to high quality OFCs is observed when increasing the modulation frequency. We have systematically observed the transition from high quality OFCs to broadened spectra at different frequencies in both the DFB laser and the DML when increasing the modulation amplitude at constant bias and when decreasing the bias at constant modulation amplitude. This behavior is illustrated in Fig. 6, where we have plotted the evolution of the two main parameters of the spectra (CNR and Δf_{10}), for both lasers at $f_m = 500$ MHz and $f_m = 5$ GHz, as a function of the gain switching conditions, V_{RF} and (I_{bias} - I_{th}). As it can be seen in Fig. 6, panels (a), (b), (e) and (f), two regimes characterized by very different CNR are clearly distinguished in separate regions of driving conditions: a regime of high CNR (40–60 dB), corresponding to coherent OFCs, and a regime of CNR ~ 0 dB, corresponding to incoherent broadened spectra. The transition between these regimes by increasing V_{RF} takes place when V_{RF} is high enough to switch off the laser, and this value depends on I_{bias} - I_{th}: the higher I_{bias}, the higher the value of V_{RF} needed to deplete the carrier density during a time long enough for the lasing photons in the cavity to be absorbed. The transition is more dramatic at $f_m = 500$ MHz than at $f_m = 5$ GHz, and for the highest bias the maximum experimental V_{RF} was not high enough to switch-off the lasers. The values and the evolution of the CNR for the DFB laser and the DML are quite similar when plotted as a function of I_{bias} - I_{th}, even though the values of the resonance frequencies are not equal in the two devices. This fact indicates that the transition between regimes is more related to the injection conditions (modulation amplitude and bias) than to the relative values of the modulation and the relaxation oscillation frequencies.

The evolution of Δf_{10} for both lasers at $f_m = 500$ MHz and $f_m = 5$ GHz as a function of the driving conditions is shown in Fig. 6(c), (d), (g), and (h). At 500 MHz and low values of V_{RF}, Δf_{10} increases with the increase of V_{RF}, taking values independent of the bias. We attribute this increment to adiabatic chirp in direct modulation regime: the changes in carrier density produce frequency modulation due to the change in the refractive index. Δf_{10} continues increasing until V_{RF} takes the values corresponding to the transition to broad noisy spectra beyond which Δf_{10} is not meaningful. The behavior is similar for $f_m = 5$ GHz, although in this case the evolution of Δf_{10} depends on the bias current. We attribute this dependence to the dependence of the relaxation oscillation frequency f_r on the bias. At low bias, f_m is close to f_r and therefore the FM efficiency is high, thus generating a spectrum that is broader than the spectrum generated at high bias, where f_m is lower than f_r and then the FM is not so significant. A detailed examination of panels (d) and (h) reveals that the evolution of Δf_{10} as a function of V_{RF} at constant I_{bias} - I_{th} is similar though not identical for both lasers. This fact is attributed to the different value of f_r for each laser.

The results in Fig. 6 are a useful guide to select the driving conditions to optimize the OFCs generated by gain switching. The best OFCs are those having high CNR and Δf_{10}. The driving conditions for generating such combs are the use of a high bias together with a high V_{RF}, but not as high as to switch-off the laser between pulses. The optimum conditions for each laser at 500 MHz and 5 GHz are marked with stars in each plot in Fig. 6. CNR around 40 (50) dB with Δf_{10} around 7 (60) GHz can be achieved at a modulation frequency of 0.5 (5) GHz. An interesting result in Fig. 6 is that both lasers exhibit the same behavior, with minimum differences, even though they have different type of cavity and phase noise properties and internal parameters. It is apparent that the driving

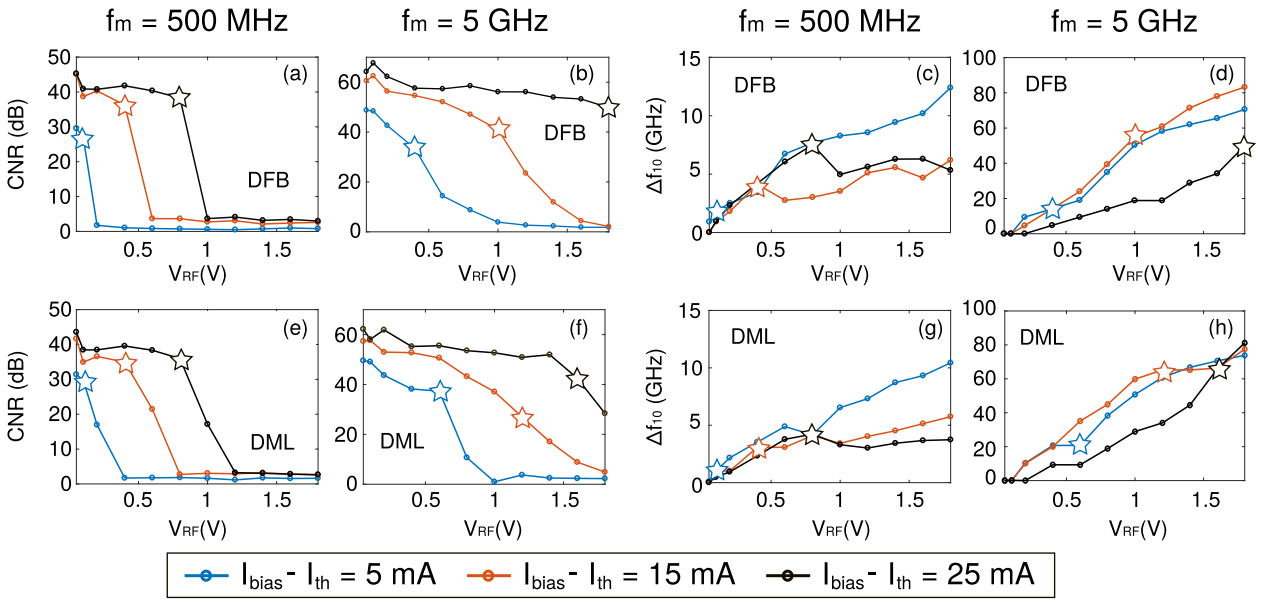

Fig. 6. Evolution of CNR and Δf_{10} as a function of the modulation amplitude V_{RF} for the DFB laser (upper row) and the DML (lower row) at $f_m = 500$ MHz (first and third columns) and $f_m = 5$ GHz (second and fourth columns) for different bias currents. The stars indicate the best comb at each bias current.

conditions are more relevant than the internal laser parameters to generate gain-switched OFCs. Additional theoretical and experimental work is still needed to properly relate the laser structure and material parameters to the quality of the OFCs generated by gain switching.

3.3. Optical injection and gain switching operation

In this section we show our results regarding the generation of OFCs by gain switching and OI as a function of the injection conditions, namely, the injected power, P_{inj}, and the detuning between the ML and the SL frequency, $\delta\nu$. A systematic study of all dynamic regimes as a function of the five operation parameters (f_m, I_{bias}, V_{RF}, P_{inj}, $\delta\nu$) is out of the scope of this work. Instead, we show some significant results obtained by changing the OI parameters in the case of the DFB laser. Similar trends were observed for other gain switching operation conditions and for the DML.

The first and second row of Fig. 7 show respectively the temporal traces and the emission spectra, when increasing the injected power into the DFB laser for small detuning, $\delta\nu = 6$ GHz. The frequency detuning, $\delta\nu$, is defined as the frequency difference between the ML and the SL emission in CW operation. We have selected operation conditions (f_m = 5 GHz, I_{bias} = 25 mA, V_{RF} = 1.8 V) producing a broad noisy spectrum without injection in order to analyze the improvement in the OFC quality with the OI. The pulses in Fig. 7(a) were obtained with very low injected power P_{inj} = −54 dBm. They show a small ringing at the pulse end, and

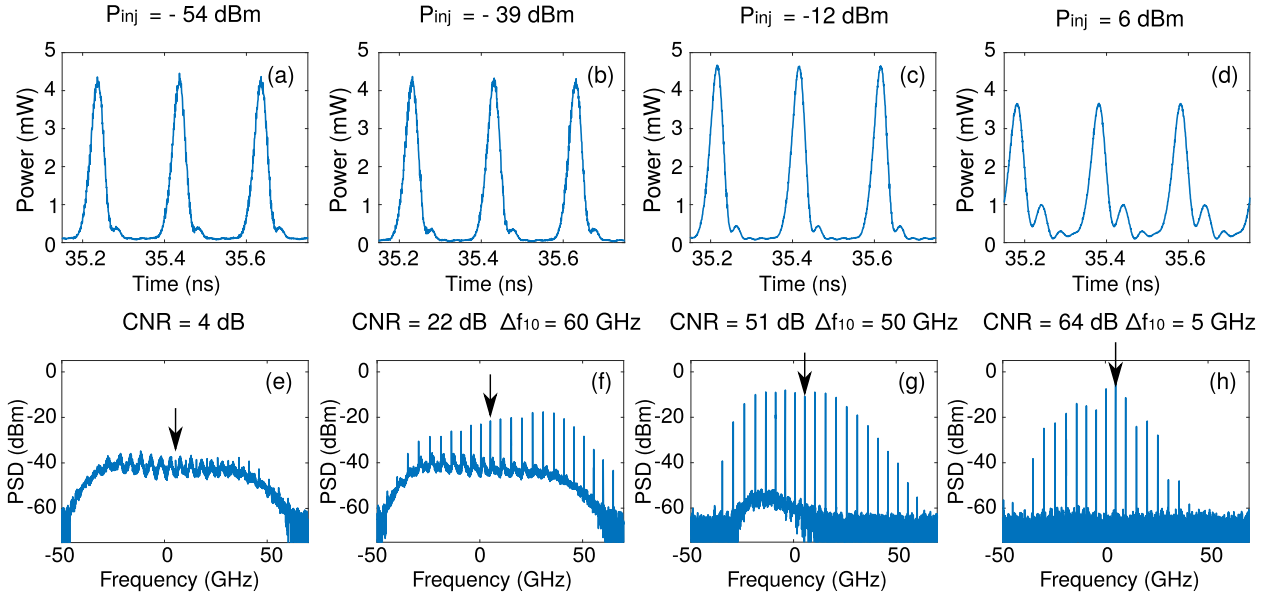

Fig. 7. Temporal traces (upper row) and optical spectra (lower row) ot the gain switched DFB laser (I_{bias} = 25 mA, f_m = 5 GHz and V_{RF} = 1.8 V) under several power levels of OI at $\delta\nu = 6$ GHz. The injection frequency is indicated with an arrow. The frequencies of the spectra are relative to the emission frequency of the free-running SL in CW operation. The injection power levels, the CNR and the Δf_{10} are labelled on top of the plots.

the corresponding spectrum in Fig. 7(e) does not show clear comb lines, although very small peaks at frequencies separated from the ML frequency by multiples of f_m are visible. This corresponds to the absence of locking and the generation of uncoherent pulses together with the modulation of the injected signal by the carrier dynamics. When increasing the injected power as in Fig. 7(b) and (f), the temporal shape is similar to the previous one, but the spectrum shows clear tones with CNR =22 dB, indicating clear locking. However, the noise level is still high due to the competition of the spontaneous emission and the injected field to build up the emitted pulses. At higher injected power (Fig. 7(c) and (g)), the temporal shape of the pulses remains similar, but now the spectrum is very flat and broad with a high CNR of 51 dB and 10 lines in 10 dB. These are the best injection conditions for generating a high quality OFC from the non-injected broad spectrum. At a higher injection level (P_{inj} = 6 dBm) the optical pulses present clear ringing (Fig. 7(d)) and the spectrum shows a high CNR but a narrower width, Δf_{10} = 5 GHz, as well as poor flatness.

Fig. 8 shows the influence of the detuning $\delta\nu$, on the comb generated under switching conditions (f_m = 5 GHz, I_{bias} = 15 mA, V_{RF} = 1.6 V) slightly different than those of Fig. 7. At very high positive or negative detuning, as shown in Fig. 8(a) for $\delta\nu$ =55 GHz, the emission spectra do not show comb lines but a broad noisy emission together with the ML line and the side bands due to the gain modulation. For a relatively broad range of detuning (-30 GHz $< \delta\nu <$ 30 GHz) the SL is locked to the ML and the spectra correspond to OFCs with high CNR and wide Δf_{10} (Fig. 8(b) and (c)). At some particular injection conditions, for instance at $\delta\nu = -37$ GHz (Fig. 8(d)), the optical spectrum shows double period dynamics.

The improvement by OI of the quality of the OFC (defined in terms of the number of harmonics with high CNR) have been previously reported theoretical [31,34] and experimentally [30]. However, this is not a general rule. As we have just shown, a broad incoherent spectrum can be transformed into a high quality OFC by OI, but the properties of a gain switching OFC can also deteriorate by OI. Fig. 9 is an illustrative example of this behavior. It shows the evolution of a high quality OFC generated by the DFB laser at 5 GHz when increasing the OI power. The non-injected spectrum (Fig. 9(a)) exhibits a high CNR = 43 dB, with broad Δf_{10} = 60 GHz. When a relatively low power (-39 dBm) is injected at a detuning of $\delta\nu$ =5 GHz, the SL is not locked to the ML and two overlapped combs, with a slight shift between them, appear (Fig. 9(b)). One of the combs corresponds to the SL while the second is due to the injected power which is amplified and emitted according to the carrier dynamics, thus producing the second comb. This behaviour was theoretical predicted in [34]. When the injected power is increased, as shown in Fig. 9(c), the SL is locked to the ML and a comb is built around the ML wavelength. In addition, at these particular driving and injection conditions, the weak lines between the comb tones may be indicative of a period doubling dynamics. At a high injection level of -3 dBm, the spectrum becomes very complex (Fig. 9(d)). It consist of tones at 1 GHz (five times the period), with an irregular intensity distribution over a high noise floor. This kind of spectrum has not been previously reported neither theoretically nor experimentally, as far as we know. Apart from this illustrative example of the worsening of the comb quality by OI, we have observed many other types of anomalous emission spectra which descriptions are out of the scope of this work.

A clear advantage of the OI for the generation of OFCs is the reduction of the phase noise. This effect is evidenced by the transferring of the narrow linewidth of the ML to each comb line of the SL. This improvement has been experimentally demonstrated by different authors [30,33,23], as well as theoretically studied [34]. We have observed the same trend in both, the DML and the DFB laser in locking conditions. Fig. 10 compares the CW lineshape of the DFB laser in free-running (I_{bias} = 30 mA) and under OI (P_{inj} = 6 dBm; $\delta\nu = -1$ GHz), measured using the DSH technique. The linewidth is reduced from around 600 kHz to around 75 kHz, which is the measured linewidth of the ML. Same behavior has been observed in the linewidth of each peak of the gain-switched OFCs,

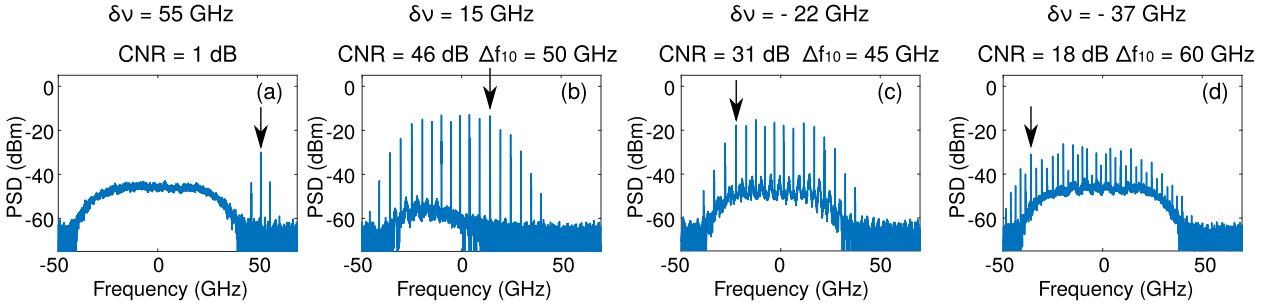

Fig. 8. Optical spectra of the gain-switched DFB laser (I_{bias} = 15 mA, f_m = 5 GHz and V_{RF} = 1.6 V) under OI ($P_{inj} = -24$ dBm) at several detuning frequencies. The arrows indicate the injection frequency relative to the SL emission in CW operation. The CNR and $\delta\nu$ are labelled on top of the plots.

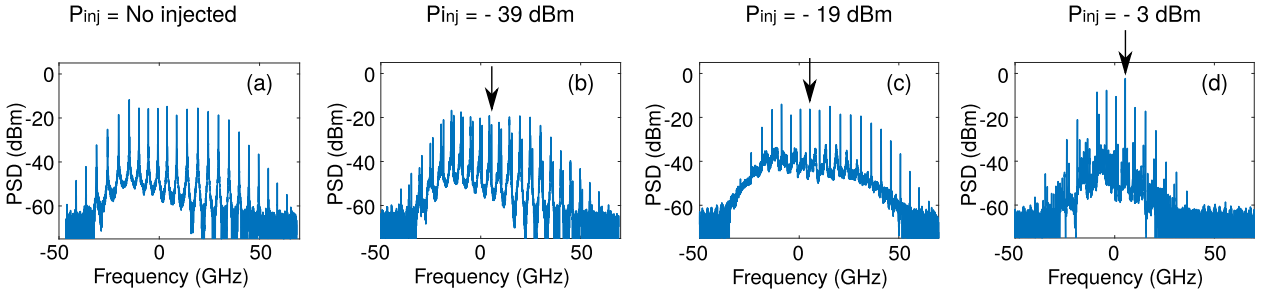

Fig. 9. Optical spectra of the gain-switched DFB laser (f_m = 5 GHz, I_{bias} = 25 mA, V_{RF} = 1 V), under several power levels of OI at $\delta\nu$ = 5 GHz. The arrows indicates the injection frequency relative to the SL emission in CW operation. The injection power levels are labelled on top of the plots.

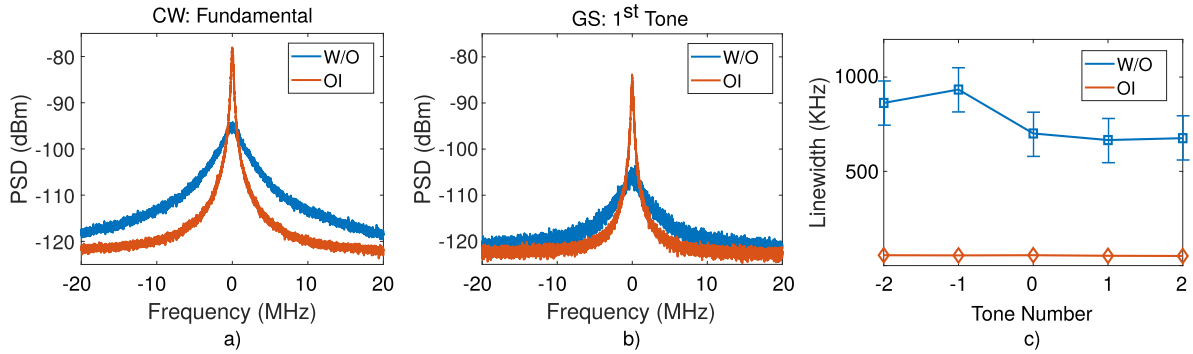

Fig. 10. RF spectra of the DSH signal of the DFB laser with and without OI, (a) CW lineshape for $I_{bias} = 30$ mA. (b) Lineshape of the 1st tone of the OFC ($I_{bias} = 30$ mA, $V_{RF} = 1$ V, $f_r = 5$ GHz). (c) Linewidths of the first 5 tones of the OFC. For all panels, without OI is indicated in blue and with OI in red ($P_{inj} = 6$ dBm, $\delta\nu = -1$ GHz). (For interpretation of the references to colour in this figure legend, the reader is referred to the web version of this article.)

as it is shown in Fig. 10(b), where the lineshapes of the central lines of the non-injected and the optically injected combs are compared (I_{bias} = 30 mA, V_{RF} = 1 V, f_m = 5 GHz). The linewidth reduction caused by the OI is noticeable. Finally, Fig. 10(c) compares the measured linewidths of the different tones of the OFCs in non-injection and injection conditions, showing a reduction around a factor ten.

4. Conclusion

The combined systematic analysis of the temporal profiles and the RF and optical spectra of the OFCs generated by gain switching under a wide range of driving conditions has provided a clear understanding of the relationship between the driving conditions and the comb characteristics in terms of dynamic and adiabatic chirp. It has been confirmed that the driving conditions leading to high quality OFCs are a high bias and the highest modulation voltage such that the laser is not completely switched-off between pulses. The transition between high quality coherent combs and broad incoherent spectra is abrupt and takes place by decreasing the bias at constant modulation voltage or by increasing the modulation voltage at constant bias. We have demonstrated that the driving conditions are more influential in the comb quality than the type of cavity or other internal parameters of the laser. Our results provide a useful guide for selecting the suitable driving conditions for specific comb characteristics. Finally we have confirmed the improvement of the OFC quality by OI but have also shown the degradation of the quality under OI in a large range of injection conditions.

Acknowledgment

This work was funded by the Ministerio de Economia y Competitividad of Spain (COMBINA, TEC201565212-C3-1-P and TEC201565212-C3-2-P). A.R., A.P., J.M.G.T. and I.E. also acknowledge support from the Comunidad de Madrid (SINFOTON-CM, S2013/MIT-2790).

References

[1] T. Rosenband, D.B. Hume, P.O. Schmidt, C.W. Chou, A. Brusch, L. Lorini, W.H. Oskay, R.E. Drullinger, T.M. Fortier, J.E. Stalnaker, S.A. Diddams, W.C. Swann, N. R. Newbury, W.M. Itano, D.J. Wineland, J.C. Bergquist, Frequency ratio of Al+ and Hg+ single-ion optical clocks; metrology at the 17th decimal place, Science 319 (5871) (2008) 1808–1812.
[2] V. Torres-Company, A.M. Weiner, Optical frequency comb technology for ultra-broadband radio-frequency photonics, Laser Photon. Rev. 8 (2014) 368–393.
[3] P. Peng, R. Shiu, M. Bitew, T. Chang, C. Lai, J. Junior, A 12 GHz wavelength spacing multi-wavelength laser source for wireless communication systems, Opt. Laser Technol. 93 (2017) 175–179.
[4] M. Imran, P.M. Anandarajah, A. Kaszubowska-Anandarajah, N. Sambo, L. Poti, A survey of optical carrier generation techniques for terabit capacity elastic optical networks, IEEE Commun. Surv. Tutor. 20 (1) (2018) 211–263.
[5] I. Coddington, N. Newbury, W. Swann, Dual-comb spectroscopy, Optica 3 (2016) 414.
[6] S.T. Cundiff, A.M. Weiner, Optical arbitrary waveform generation, Nat. Photon. 4 (11) (2010) 760.
[7] I. Coddington, W.C. Swann, L. Nenadovic, N.R. Newbury, Rapid and precise absolute distance measurements at long range, Nat. Photon. 3 (2009) 351–356.
[8] H. Ito, H. Yokoyama, S. Murata, H. Inaba, Picosecond optical pulse generation from an r.f. modulated AlGaAs d.h. diode laser, Electron. Lett. 15 (23) (1979) 738.
[9] S. Tarucha, K. Otsuka, Response of semiconductor laser to deep sinusoidal injection current modulation, IEEE J. Quant. Electron. 17 (5) (1981) 810–816.
[10] P.M. Anandarajah, A.M. Clarke, C. Guignard, L. Bramerie, L.P. Barry, J.D. Harvey, J.C. Simon, System-performance analysis of optimized gain-switched pulse source employed in 40- and 80-gb/s OTDM systems, J. Lightwave Technol. 25 (2007) 1495–1502.
[11] P.M. Anandarajah, K. Shi, J. O'Carroll, A. Kaszubowska, R. Phelan, L.P. Barry, A.D. Ellis, P. Perry, D. Reid, B. Kelly, J. O'Gorman, Phase shift keyed systems based on a gain switched laser transmitter, Opt. Exp. 17 (2009) 12668.
[12] M. Yoshino, N. Miki, N. Yoshimoto, K. Kumozaki, Multiwavelength optical source for OCDM using sinusoidally modulated laser diode, J. Lightwave Technol. 27 (2009) 4524–4529.
[13] P.C. Peng, K.C. Shiu, Y.M. Chen, M.A. Bitew, W.Y. Lee, C.H. Lai, Y.W. Peng, Multiwavelength laser module based on distribute feedback laser diode for broadcast and communication systems, IEEE Photon. J. 8 (2016) 1–8.
[14] B. Jerez, P. Martín-Mateos, E. Prior, C. de Dios, P. Acedo, Dual optical frequency comb architecture with capabilities from visible to mid-infrared, Opt. Exp. 24 (2016) 14986.
[15] T. Shao, R. Zhou, M.D.G. Pascual, P.M. Anandarajah, L.P. Barry, Integrated gain switched comb source for 100 gb/s WDM-SSB-DD-OFDM system, J. Lightwave Technol. 33 (2015) 3525–3532.
[16] M.D. Gutierrez Pascual, V. Vujicic, J. Braddell, F. Smyth, P.M. Anandarajah, L.P. Barry, InP photonic integrated externally injected gain switched optical frequency comb, Opt. Lett. 42 (2017) 555.
[17] M.D.G. Pascual, V. Vujicic, J. Braddell, F. Smyth, P. Anandarajah, L. Barry, Photonic integrated gain switched optical frequency comb for spectrally efficient optical transmission systems, IEEE Photon. J. 9 (2017) 1–8.
[18] A.R.C. Serrano, C. de Dios Fernandez, E.P. Cano, M. Ortsiefer, P. Meissner, P. Acedo, VCSEL-based optical frequency combs: toward efficient single-device comb generation, IEEE Photon. Technol. Lett. 25 (2013) 1981–1984.
[19] E.P. Cano, C. de Dios Fernandez, A.R.C. Serrano, M. Ortsiefer, P. Meissner, P. Acedo, Experimental study of VCSEL-based optical frequency comb generators, IEEE Photon. Technol. Lett. 26 (2014) 2118–2121.
[20] E. Prior, C. de Dios, A.R. Criado, M. Ortsiefer, P. Meissner, P. Acedo, Expansion of VCSEL-based optical frequency combs in the sub-THz span: Comparison of non-linear techniques, J. Lightwave Technol. 34 (2016) 4135–4142.
[21] E. Prior, C. De Dios, M. Ortsiefer, P. Meissner, P. Acedo, Understanding VCSEL-based gain switching optical frequency combs: experimental study of polarization dynamics, J. Lightwave Technol. 33 (2015) 4572–4579.
[22] A. Quirce, C. de Dios, A. Valle, L. Pesquera, P. Acedo, Polarization dynamics in VCSEL-based gain switching optical frequency combs, J. Lightwave Technol. 36 (2018) 1798–1806.
[23] R. Zhou, T.N. Huynh, V. Vujicic, P.M. Anandarajah, L.P. Barry, Phase noise analysis of injected gain switched comb source for coherent communications, Opt. Exp. 22 (2014) 8120.
[24] V. Vujicic, P.M. Anandarajah, R. Zhou, C. Browning, L.P. Barry, Performance investigation of IM/DD compatible SSB-OFDM systems based on optical multicarrier sources, IEEE Photon. J. 6 (2014) 1–10.
[25] T. Shao, E. Martin, A.M. Prince, L.P. Barry, DM-DD OFDM-RoF system with adaptive modulation using a gain-switched laser, IEEE Photon. Technol. Lett. 27 (2015) 856–859.

[26] M.D.G. Pascual, R. Zhou, F. Smyth, P.M. Anandarajah, L.P. Barry, Software reconfigurable highly flexible gain switched optical frequency comb source, Opt. Exp. 23 (2015) 23225.
[27] P.M. Anandarajah, S.P.O. Duill, Rui Zhou, L.P. Barry, Enhanced optical comb generation by gain-switching a single-mode semiconductor laser close to its relaxation oscillation frequency, IEEE J. Sel. Top. Quant. Electron. 21 (2015) 592–600.
[28] S. Wieczorek, B. Krauskopf, T.B. Simpson, D. Lenstra, The dynamical complexity of optically injected semiconductor lasers, Phys. Rep. 416 (1-2) (2005) 1–128.
[29] H. Zhu, R. Wang, T. Pu, P. Xiang, J. Zheng, T. Fang, A novel approach for generating flat optical frequency comb based on externally injected gain-switching distributed feedback semiconductor laser, Laser Phys. Lett. 14 (2017) 026201.
[30] P.M. Anandarajah, R. Maher, Y.Q. Xu, S. Latkowski, J. O'Carroll, S.G. Murdoch, R. Phelan, J. O'Gorman, L.P. Barry, Generation of coherent multicarrier signals by gain switching of discrete mode lasers, IEEE Photon. J. 3 (2011) 112–122.
[31] S.P. O Duill, R. Zhou, P.M. Anandarajah, L.P. Barry, Analytical approach to assess the impact of pulse-to-pulse phase coherence of optical frequency combs, IEEE J. Quant. Electron. 51 (2015) 1–8.
[32] P. Anandarajah, R. Zhou, R. Maher, D.M.G. Pascual, F. Smyth, V. Vujicic, and L. Barry, Flexible optical comb source for super channel systems," in: Optical Fiber Communication Conference/National Fiber Optic Engineers Conference 2013, OSA, 2013.
[33] R. Zhou, S. Latkowski, J. O'Carroll, R. Phelan, L.P. Barry, P. Anandarajah, 40 nm wavelength tunable gain-switched optical comb source, Opt. Exp. 19 (2011) B415.
[34] S.P. Ó Dúill, P.M. Anandarajah, R. Zhou, L.P. Barry, Numerical investigation into the injection-locking phenomena of gain switched lasers for optical frequency comb generation, Appl. Phys. Lett. 106 (2015) 211105.
[35] T. Okoshi, K. Kikuchi, A. Nakayama, Novel method for high resolution measurement of laser output spectrum, Electron. Lett. 16 (16) (1980) 630.
[36] M. Vilera, A. Pérez-Serrano, M. Faugeron, J.M.G. Tijero, M. Krakowski, F. van Dijk, I. Esquivias, Modulation performance of three-section integrated mopas for pseudorandom lidar, IEEE Photon. Technol. Lett. 29 (17) (2017) 1486–1489.
[37] L.A. Coldren, S.W. Corzine, M.I. Masanovic, Diode Lasers and Photonic Integrated Circuits, 2012.
[38] D.A. Leep, D.A. Holm, Spectral measurement of timing jitter in gain-switched semiconductor lasers, Appl. Phys. Lett. 60 (1992) 2451–2453.
[39] M. Jinno, Correlated and uncorrelated timing jitter in gain-switched laser diodes, IEEE Photon.Technol. Lett. 5 (10) (1993) 1140–1143.
[40] S. Kobayashi, Y. Yamamoto, M. Ito, T. Kimura, Direct frequency modulation in AlGaAs semiconductor lasers, IEEE J. Quant. Electron. 18 (4) (1982) 582–595.
[41] P. Corvini, T. Koch, Computer simulation of high-bit-rate optical fiber transmission using single-frequency lasers, J. Lightwave Technol. 5 (11) (1987) 1591–1595.
[42] A. Consoli, J.M.G. Tijero, I. Esquivias, Time resolved chirp measurements of gain switched semiconductor laser using a polarization based optical differentiator, Opt. Exp. 19 (2011) 10805.
[43] C. Guignard, P. Anandarajah, A. Clarke, L. Barry, O. Vaudel, P. Besnard, Experimental investigation of the impact of optical injection on vital parameters of a gain-switched pulse source, Opt. Commun. 277 (2007) 150–155.
[44] P. Anandarajah, P. Perry, C. Herbert, D. Jones, A. Kaszubowska-Anandarajah, L. Barry, B. Kelly, J. O'Carroll, J. O'Gorman, M. Rensing, R. Phelan, Discrete mode lasers for communication applications, IET Optoelectron. 3 (2009) 1–17.